

*Title*

**“Low-temperature sintering of Z-type hexagonal ferrite by addition of fluorine containing glass powder”**

*Author's Name*

**Yasutaka MIZUNO, Seiichi TARUTA and Kunio KITAJIMA**

*Author's Affiliation*

**Department of Chemical and Materials Engineering, Faculty of Engineering,  
Shinshu University, 4-17-1, Wakasato, Nagano-shi, Nagano, 380-8553, Japan**

*Corresponding Author*

**Seiichi TARUTA**

**Department of Chemical and Materials Engineering, Faculty of Engineering,  
Shinshu University,**

**4-17-1, Wakasato, Nagano-shi, Nagano, 380-8553, Japan**

**TEL: +81-26-269-5416**

**FAX: +81-26-269-5424**

**E-mail: staruta@gipwc.shinshu-u.ac.jp**

## **Abstract**

In order to reduce the sintering temperature of  $\text{Ba}_3\text{Co}_2\text{Fe}_{24}\text{O}_{41}$  ( $\text{Co}_2\text{Z}$ ), fluorine containing glass powder was added as a sintering aid to ferrite powder with a  $\text{Co}_2\text{Z}$  stoichiometric composition prepared by a solid-state reaction, and dense sintered specimens could be obtained at  $1000^\circ\text{C}$  in air. The densification was achieved by liquid-phase sintering which was induced by the melting of the additive glass at  $\sim 800^\circ\text{C}$ . The main crystalline phase was  $\text{Co}_2\text{Z}$ , and spinel ferrite appeared as the impurity phase. By sintering in a sealed container, the densification was accelerated still more, and in addition to spinel ferrite, Ba-M also appeared as the impurity phase. The Ba-M contained some Co instead of Fe, and grew to discontinuously large hexagonal plate-like grains. In a fluorine and/or fluorides rich atmosphere,  $\text{Co}_2\text{Z}$  was decomposed to Ba-M and spinel ferrite, and large hexagonal plate-like grains appeared. These results suggest that fluorine and/or fluorides evaporated from the additive glass decomposed  $\text{Co}_2\text{Z}$  to Ba-M and spinel ferrite, and induced the discontinuously grain growth of Ba-M. The initial permeability was lower than that of the specimen with no additive glass but remained almost constant in the frequency regions up to 1 GHz.

## **Key-Words**

Z-type hexagonal ferrite, Liquid-phase sintering, Fluorine containing glass powder, Solid-state reaction, Initial permeability

## 1. Introduction

The hexagonal ferrites are the groups of ferromagnetic compounds discovered by Philips at 1952-1956. As the typical hexagonal ferrites, there are M type ( $\text{BaFe}_{12}\text{O}_{19}$ ; Ba-M), Y type ( $\text{Ba}_2\text{Co}_2\text{Fe}_{12}\text{O}_{22}$ ;  $\text{Co}_2\text{Y}$ ), W type ( $\text{BaCo}_2\text{Fe}_{16}\text{O}_{27}$ ;  $\text{Co}_2\text{W}$ ) and Z type ( $\text{Ba}_3\text{Co}_2\text{Fe}_{24}\text{O}_{41}$ ;  $\text{Co}_2\text{Z}$ ) [1,2]. Among these ferrites,  $\text{Co}_2\text{Z}$  has a high initial permeability in frequency regions higher than 300 MHz [2]. On the other hand, NiCuZn spinel ferrites are now commercially used for multi-layer chip inductors (MLCI), but cannot be used in such high frequency regions. Therefore, it is expected that  $\text{Co}_2\text{Z}$  can be used in high frequency regions of electronic devices such as MLCI. MLCI is produced by co-firing multi-layered NiZnCu spinel ferrites with an internal electrode such as copper or silver which are relatively cheap and good electrical conductors. If  $\text{Co}_2\text{Z}$  is applied to MLCI with a copper internal electrode, it must be sintered at  $\leq 1000^\circ\text{C}$ . However, presently, this is difficult [3,4], so Z type hexagonal ferrites with Sr, Cu or Pb substituted for Ba and Co in  $\text{Co}_2\text{Z}$  are synthesized [3,5-7]. Though their sintering temperatures are lower than that of stoichiometric  $\text{Co}_2\text{Z}$ , they must be sintered at  $> 1100^\circ\text{C}$  to be densified [3,5-7].

In this work, we proposed a densification technique of  $\text{Co}_2\text{Z}$  at lower sintering temperatures. As a sintering aid, a fluorine containing glass powder, of which the chemical composition is shown in Table I, was added to  $\text{Co}_2\text{Z}$  powder prepared by the solid-state reaction. The powder mixture was sintered in air or in a sealed platinum container. The influences of the glass addition and the sintering condition on the densification, phase change and microstructure development were

investigated. Furthermore,  $\text{Co}_2\text{Z}$  powder, to which the additive glass powder was not added, was sintered together with the additive glass or fluoride ( $\text{MgF}_2$  or  $\text{LiF}$ ) powder pellet in the sealed platinum container. Also, the influence of fluorine and/or fluoride evaporated from such powder pellets on the crystalline phases and microstructure development was investigated.

## 2. Experimental procedure

### 2.1 Preparation of additive glass and ferrite powders

The reagents of  $\text{Li}_2\text{CO}_3$ ,  $\text{K}_2\text{CO}_3$ ,  $\text{SrCO}_3$ ,  $\text{CaCO}_3$ ,  $\text{MgO}$ ,  $\text{SiO}_2$ ,  $\text{CaF}_2$  and  $\text{Al}_2\text{O}_3$  were used as starting materials of the additive glass with the chemical composition shown in Table I, mixed and calcined at  $900^\circ\text{C}$  for 1 h. The mixture was then melted in a sealed platinum container at  $1450^\circ\text{C}$  for 2 h and cooled rapidly in cold water. The resulting glass was ground using an alumina mortar, passed through a 100-mesh sieve and subsequently, pulverized by ball-milling in ethanol using a zirconia jar and balls. The average particle size of the resulting additive glass powder was  $\sim 0.52 \mu\text{m}$ .

The ferrite was prepared by the traditional solid-state reaction method. The reagents of  $\text{BaCO}_3$ ,  $\text{CoO}$ , and  $\text{Fe}_2\text{O}_3$  were mixed in the ratio corresponding to the stoichiometric  $\text{Co}_2\text{Z}$  ( $\text{Ba}_3\text{Co}_2\text{Fe}_{24}\text{O}_{41}$ ) by ball-milling for 8 h. The mixture was calcined in air at  $1300^\circ\text{C}$  for 10 h, ground using an alumina mortar, and passed through a 100-mesh sieve.

## 2.2 Preparation and characterization of sintered specimens

The obtained ferrite and additive glass powders were mixed by ball-milling for 48 h in ethanol using a zirconia jar and balls. The content of the additive glass powder was 5 mass%. The powder mixture was passed through a 100-mesh sieve, and compacted to 9 mm diameter and 2 mm thickness by cold isostatic pressing at 98 MPa. Toroidal powder compacts of 9 mm outer diameter, 4.5 mm inner diameter, and 2.5 mm in thickness were also prepared in the same way, and were used for the evaluation of initial permeability. The powder compacts were sintered in air or in a sealed platinum container. To compare the 0 % glass added-specimen with the 5 % glass added-specimen, the 0 % glass added-specimen was prepared in the same way, and was sintered together with the additive glass,  $\text{MgF}_2$  or LiF powder pellet in the sealed platinum container. When fluoride such as  $\text{MgF}_2$  and LiF was heated in such a manner, a fluorine and/or fluoride rich atmosphere was intentionally achieved.

Thermal properties of the additive glass were analyzed using a differential thermal analyzer (DTA: DTG-50, Shimadzu, Japan) with a heating rate of  $10^\circ\text{C}/\text{min}$ . Crystalline phases of the as-calcined ferrite powder and the sintered specimens were identified using an X-ray diffractometer (XRD: XRD-6000, Shimadzu, Japan). Relative densities of the sintered specimens were calculated from the bulk and true densities. The bulk densities were measured by the Archimedes method. The true densities were calculated from the true density of the additive glass measured by the pycnometer method and the theoretical density of  $\text{Co}_2\text{Z}$ . Fractured surfaces of the sintered specimens were observed using a field-emission scanning electron

microscope (SEM: S-4100, Hitachi, Japan). A quantitative analysis of the elements in the sintered specimens was made using an electron probe micro analyzer (EPMA: JXA-8100, JEOL, Japan). The initial permeability of the sintered specimens was measured at room temperatures using an impedance analyzer (HP4291B, Hewlett Packard).

### 3. Results and discussion

#### 3.1 Densification behavior

DTA curve of the additive glass is shown in Fig. 1. Two strong exothermic peaks at 494°C ( $T_{c1}$ ) and 567°C ( $T_{c2}$ ), and an endothermic peak at about 800°C ( $T_m$ ) were observed.  $T_m$  was attributed to the melting of the glass, so the additive glass powder was heated at 1000°C for 1 h and cooled rapidly. As a result, a clear bulk glass was obtained, and crystal peaks were not observed in its XRD pattern. Even if crystalline phases were separated from the additive glass at 494°C ( $T_{c1}$ ) and 567°C ( $T_{c2}$ ), they would all have turned to liquid phase at 1000°C. These results suggest that this additive glass was suitable as a sintering aid for  $\text{Co}_2\text{Z}$  ferrite production at  $\leq 1000^\circ\text{C}$ .

Bulk and relative densities of the sintered specimens are shown in Table II. It is clear that by the 5 mass% addition of the glass powder, the densification of the specimen was promoted. This was achieved by liquid-phase sintering which was induced by the melting of the additive glass at  $\sim 800^\circ\text{C}$ . The relative density of the 5 % glass added-specimen reached  $\sim 93\%$  at 1000°C for 1 h. When the sintering time

was extended to 10 h at 1000°C, the bulk density stayed almost constant. Consequently, the densification was terminated at 1000°C for 1 h. Also, by sintering in the sealed platinum container, the densification was accelerated still more.

### 3.2 Crystalline phase

XRD patterns of the as-calcined ferrite powder and the 0 % glass added-specimen are shown in Fig. 2.  $\text{Co}_2\text{Z}$  was the main crystalline phase in the as-calcined ferrite powder, and  $\text{Co}_2\text{Y}$  and  $\text{Co}_2\text{W}$  were observed as the impurity phases (Fig. 2 (a)). Though the characteristic peaks of Ba-M, which should appear at 32.1° and 34.0°, could not be confirmed, a small peak of Ba-M was observed near 23.0°. By sintering at 1000°C in air or in the sealed container, the characteristic peaks of Ba-M appeared and the peaks of  $\text{Co}_2\text{Y}$  and  $\text{Co}_2\text{W}$  disappeared (Fig. 2 (b) and (c)). Furthermore, in the XRD patterns measured at a slow scanning rate (Fig. 3 (a) and (b)), the peaks of Ba-M were observed near 19.0° and 23.0°. At 1300°C, the peaks of Ba-M became very small and  $\text{Co}_2\text{Y}$  and  $\text{Co}_2\text{W}$  appeared again (Fig. 2 (d)).

$\text{Co}_2\text{Z}$  always coexisted with Ba-M in the 0 % glass added-specimen in this study and, in an other study [8], coexisted with Y, W and M type ferrites and  $\text{Ba}_2\text{Fe}_2\text{O}_5$  at 1200-1300°C. Furthermore, there are reports [3,4] that a single phase of  $\text{Co}_2\text{Z}$  is obtained at 1200-1300°C. The difference between this study and the other reports, in which a single phase of  $\text{Co}_2\text{Z}$  was obtained, was the purity of  $\text{Fe}_2\text{O}_3$  used as reagent [3] and the sintering atmosphere [4]. The purity of  $\text{Fe}_2\text{O}_3$  was 98 % in this study, which was lower than that of  $\text{Fe}_2\text{O}_3$  used in the other reports (99.4% [3] and 99.9%

[4]). Also, a single phase of  $\text{Co}_2\text{Z}$  was obtained in the  $\text{O}_2$  atmosphere [4]. Furthermore, it was reported that the formation of the hexagonal ferrites depended on the sintering condition and the additive content [5-7]. These results suggest that the formation of impurity phases such as Y, W and M type ferrites might depend on the purity of starting materials, the kind of the additive, and the sintering condition.

XRD patterns of the 5 % glass added-specimen are shown in Fig. 4.  $\text{Co}_2\text{Z}$  was the main crystalline phase in the specimens sintered at both  $975^\circ\text{C}$  and  $1000^\circ\text{C}$  in air, and spinel ferrite was also observed as impurity phase (Fig. 4 (a) and (b)). Spinel ferrite might be  $\text{CoFe}_2\text{O}_4$  or  $\gamma\text{-Fe}_2\text{O}_3$ , according to the JCPDS cards. Zhang et al. [7] reported that spinel ferrite was observed in the sintered specimens of Z type hexagonal ferrite with Cu, and also with Zn substituted for Co in  $\text{Co}_2\text{Z}$ . The characteristic peaks of Ba-M ( $19.0^\circ$ ,  $23.0^\circ$ ,  $32.1^\circ$  and  $34.0^\circ$ ) were not observed in the specimens sintered at either  $975^\circ\text{C}$  or  $1000^\circ\text{C}$  for 1 h in air (Fig. 3 (c), Fig. 4 (a) and (b)). By sintering at  $1000^\circ\text{C}$  for 10 h in the sealed container or at  $1050^\circ\text{C}$  for 1 h in air, the characteristic peaks of Ba-M appeared (Fig. 3 (d), Fig. 4 (c) and (d)).

The above results show that by 5 mass% addition of the glass powder used in this study, the dense sintered specimens, in which  $\text{Co}_2\text{Z}$  was the main crystalline phase, were obtained at  $1000^\circ\text{C}$ . However, spinel ferrite was formed as an impurity phase. By sintering at  $1000^\circ\text{C}$  for long time in the sealed container or at  $1050^\circ\text{C}$  in air, Ba-M was formed and the quantity of spinel ferrite increased. These results indicate that the addition of fluorine containing glass brought about the decomposition of  $\text{Co}_2\text{Z}$ . The details of the influence of the glass addition are discussed later.



### 3.3 Microstructure development

SEM photographs of fractured surfaces of the 0 % glass and the 5 % glass added-specimens are shown in Fig. 5. The grains of the 5 % glass added-specimen sintered at 1000°C for 1 h in air were  $<0.5 \mu\text{m}$  (Fig. 5 (a)). By sintering at 1000°C for 10 h in the sealed container, discontinuously grown hexagonal plate-like grains  $\sim 3 \mu\text{m}$  were observed in the matrix of fine sub-micron grains (Fig. 5 (b)). The discontinuous grain growth is felt to have been induced by the addition of the glass powder because it was not observed in the 0 % glass added-specimen (Fig. 5 (c)).

The chemical compositions of both the discontinuously grown grains and the fine grains were analyzed using EPMA. The reflection electron image and distributions of Ba, Co and Fe on a polished surface of the 5 % glass added-specimen sintered at 1000°C for 10 h in the sealed container are shown in Fig. 6. The contrast in Fig. 6 (b), (c) and (d) means that the brighter part is richer in the element. In the discontinuously grown grains, the concentrations of Ba and Co were relatively low, and that of Fe was high, compared with that of the corresponding elements in the fine grains. The results of the quantitative analysis for the discontinuously grown grains and the fine grains using EPMA are shown in Table III with the quantity of elements in the stoichiometric  $\text{Co}_2\text{Z}$  and Ba-M. The composition of the fine grains almost coincided with that of  $\text{Co}_2\text{Z}$ . The concentration of Fe in the discontinuously grown grains was relatively low, compared with Fe content in stoichiometric Ba-M. The detected quantity of Co was close to the quantity of the missing Fe in the

discontinuously grown grains, which was assumed to be Ba-M. That is, the discontinuously grown grains were Ba-M ( $\text{BaFe}_{11.65}\text{Co}_{0.35}\text{O}_{19}$ ) in which Fe was partially replaced with Co.

### 3.4 Influence of fluorine and/or fluorides on crystalline phase formation and microstructure development

In order to clarify the origin of the discontinuous grain growth, we focused on fluorine and fluorides in the additive glass and investigated the influence of fluorine and/or fluorides on the sintering of  $\text{Co}_2\text{Z}$ . XRD patterns of the 0 % glass added-specimen sintered at  $1000^\circ\text{C}$  for 10 h together with the additive glass powder or  $\text{MgF}_2$  powder pellet in the sealed container are shown in Fig. 7. By sintering in the atmosphere where  $\text{MgF}_2$  was volatilized and/or decomposed into  $\text{F}_2$  gas,  $\text{Co}_2\text{Z}$  did not exist at all, and Ba-M,  $\text{BaF}_2$  and spinel ferrite appeared (Fig. 7 (b)). By sintering together with a  $\text{LiF}$  powder pellet in the sealed container, Ba-M and spinel ferrite were observed in the XRD pattern, and  $\text{LiF}$  vanished due to decomposition or evaporation during the firing. These results show that fluorine,  $\text{MgF}_2$  and/or  $\text{LiF}_2$  decomposed  $\text{Co}_2\text{Z}$  into Ba-M and spinel ferrite. By sintering together with the additive glass powder pellet in the sealed container, not only  $\text{Co}_2\text{Z}$  but also Ba-M and spinel ferrite were observed (Fig. 7 (a)). The above results suggest that fluorine and/or fluorides such as  $\text{MgF}_2$  and  $\text{LiF}$ , which were evaporated from the additive glass, decomposed  $\text{Co}_2\text{Z}$  into Ba-M and spinel ferrite. The formation of Ba-M and spinel ferrite was accelerated by the sintering in the sealed container or at a higher

temperature because fluorine and/or fluorides existed abundantly on such sintering conditions. Figure 8 is an SEM photograph of the 0 % glass added-specimen sintered at 1000°C for 10 h together with MgF<sub>2</sub> powder pellet in the sealed container. While most grains were <1 μm in size, many hexagonal plate-like grains with size of ~5 μm were observed. This indicates that fluorine and/or fluorides induced the discontinuous grain growth of Ba-M.

### 3.5 Permeability of sintered specimens

Real and imaginary parts of initial permeabilities of the 0 % glass added-specimen sintered at 1300°C for 1 h in air and the 5 % glass added-specimen sintered at 1000°C for 1 h in air are shown in Fig. 9. The real part of the initial permeability of the 0 % glass added-specimen decreased, and the imaginary part increased rapidly above 800 MHz. Though the real part of the initial permeability of the 5 % glass added-specimen was smaller than that of the 0 % glass added-specimen, it remained almost constant in the high frequency regions up to 1 GHz. The initial permeability ( $\mu_r' = 2.6$ ) of the 5 % glass added-specimen was almost the same as that of the dense Z type hexagonal ferrite ( $3\text{Ba}_{0.5}\text{Sr}_{0.5}\text{O} \cdot 2\text{CoO} \cdot 12\text{Fe}_2\text{O}_3$ ) with 6 mass% Bi-Zn-B glass sintered at 1050°C for 2 h [9]. The initial permeability of the Z type hexagonal ferrite ( $3\text{Ba}_{0.5}\text{Sr}_{0.5}\text{O} \cdot 2\text{CoO} \cdot 12\text{Fe}_2\text{O}_3$ ) decreased with an increase in the glass content. This may have resulted from the nonmagnetic ions by the glass entering the crystal lattice of the ferrite, thus reducing the saturation magnetization, and hence the

initial permeability [9]. The same phenomenon might have been induced in this study while the sintering temperature was lower in this study.

#### 4. Conclusion

In order to obtain dense  $\text{Co}_2\text{Z}$  at lower temperatures, the fluorine containing glass powder was added as a sintering aid to the ferrite powder with  $\text{Co}_2\text{Z}$  stoichiometric composition prepared by the traditional solid-state reaction. The dense sintered bodies, in which  $\text{Co}_2\text{Z}$  was the main crystalline phase and spinel ferrite was the impurity phase, could be obtained at  $1000^\circ\text{C}$  in air by the 5 mass% addition of the glass powder. The densification was achieved by the liquid sintering which was induced by the melting of the additive glass. By sintering in a sealed container, the densification was accelerated still more, and not only spinel ferrite but also Ba-M appeared as the impurity phase, and grew to discontinuously large hexagonal plate-like grains. In fluorine and/or fluorides rich atmosphere,  $\text{Co}_2\text{Z}$  decomposed to Ba-M and spinel ferrite, and large hexagonal plate-like grains appeared. These results suggest that fluorine and/or fluorides evaporated from the additive glass decomposed  $\text{Co}_2\text{Z}$  to Ba-M and spinel ferrite and induced the discontinuously grain growth of Ba-M. The initial permeability was lower than that of the specimen with no additive glass but remained almost constant in the frequency regions up to 1 GHz.

## **Acknowledgement**

The authors would like to thank Dr. Junichi Miyashita of Precision Technology Research Institute of Nagano Prefecture Electronic Department and Dr. Toshiro Sato of Department of Electrical and Electronic Engineering, Faculty of Engineering, Shinshu University, for the experimental support of magnetic properties.

## Reference

1. J. J. Went, G. W. Rathenau, E. W. Gorter and G. W. Van Oosterhaut, *Phil. Tech. Rev.*, **13** (1952) 194.
2. G. H. Jonker, H. P. J. Wijn and P. B. Braun, *Phil. Tech. Rev.*, **18** (1956) 145.
3. O. Kimura, M. Matsumoto and M. Itakura, *J. Jap. Soc. Pow. Metal.*, **42** (1995) 27.
4. O. Sakaguchi, T. Kagotani, D. Book, H. Nakamura, S. Sugimoto, M. Okada and M. Homma, *Mater. Trans., JIM* , **37** (1996) 878.
5. H. Zhang, J. Zhou, Z. Yue, P. Wu, L. Li and Z. Gui, *Mater. Sci. Eng.* **B65** (1999) 184.
6. X. Wang, T. Ren, L. Li, Z. Gui, S. Su, Z. Yue and J. Zhou, *J. Magn. Magn. Mater.*, **234** (2001) 255.
7. H. Zhang, L. Li, Y. Wang, J. Zhou, Z. Yue and Z. Gui, *J. Am. Ceram. Soc.*, **85** (2002) 1180.
8. M. Endo and A. Nakano, *J. Jap. Soc. Pow. Metal.*, **49** (2002) 124.
9. H.-I. Hsing and H.-H. Duh, *J. Mater. Sci.*, **36** (2001) 2081.

**Table I** Chemical composition of the additive glass used in this study (mass%)

	Li <sub>2</sub> O	K <sub>2</sub> O	MgO	SrO	Al <sub>2</sub> O <sub>3</sub>	SiO <sub>2</sub>	CaF <sub>2</sub>
Additive glass	10	10	7	7	1	46	19

**Table II** Bulk and relative densities of the 5 % glass added-specimen and the 0 % glass added-specimen

Specimen	Sintering Condition		Bulk Density (g/cm <sup>3</sup> )	Relative Density (%)
	Temp. (°C)	Time (h)		
5 % glass added-specimen	975	1	4.76	91.2
	1000	1	4.86	93.1
	1000	10	4.88	93.5
	1000	10*	5.01	96.0
0 % glass added-specimen	1050	1	4.59	85.7
	1075	1	4.93	92.2
	1100	1	5.08	95.0



**Table III** Quantitative analysis for both discontinuously grown grain and fine grains of the polished surface shown in **Fig. 6** and quantity of elements in the stoichiometric Co<sub>2</sub>Z and Ba-M

	Analysis value of elements (mass%)			
	<b>Ba</b>	<b>Fe</b>	<b>Co</b>	<b>O</b>
Discontinuously grown grain	12.6	58.7	1.2	27.1
Fine grains	16.3	51.1	4.7	26.3
	Quantity of elements in the stoichiometric composition (mass%)			
Co <sub>2</sub> Z	16.3	53.0	4.7	26.0
Ba-M	12.4	60.3		27.3

## Figure captions

**Fig. 1.** DTA curve of the additive glass.

**Fig. 2.** XRD patterns of (a) the as-calcined ferrite powder and the 0 % glass added-specimen sintered at (b) 1000°C for 1 h in air, (c) 1000°C for 10 h in the sealed platinum container and (d) 1300°C for 1 h in air. (●): Co<sub>2</sub>Z, (●): Ba-M, (○): Co<sub>2</sub>Y, (Δ): Co<sub>2</sub>W.

**Fig. 3.** XRD patterns of the 0 % glass added-specimen sintered at 1000°C (a) for 1 h in air and (b) for 10 h in the sealed platinum container and the 5 % glass added-specimen sintered at 1000°C (c) for 1 h in air and (d) for 10 h in the sealed platinum container. (●): Co<sub>2</sub>Z, (●): Ba-M, (▼): Unknown.

**Fig. 4.** XRD patterns of the 5 % glass added-specimen sintered at (a) 975°C for 1 h in air, (b) 1000 °C for 1 h in air, (c) 1000°C for 10 h in the sealed platinum container and (d) at 1050°C for 1 h in air. (●): Co<sub>2</sub>Z, (●): Ba-M, (Δ): Co<sub>2</sub>W, (■): Spinel ferrite.

**Fig. 5.** SEM photographs of fractured surfaces of the 5 % glass added-specimen sintered at 1000°C (a) for 1 h in air, (b) for 10 h in the sealed platinum container and (c) the 0 % glass added-specimen sintered at 1000°C for 10 h in the sealed platinum

container.

**Fig. 6.** (a) The reflection electron image of the polished surface of the 5 % glass added-specimen sintered at 1000°C for 10 h in the sealed platinum container. Distribution of (b) Ba, (c) Co and (d) Fe on the same surface of the sintered specimen. The contrast of (b), (c) and (d) means that the brighter part is richer in the element.

**Fig. 7.** XRD patterns of the 0 % glass added-specimen sintered at 1000°C for 10 h together with (a) the additive glass powder pellet and (b) MgF<sub>2</sub> powder pellet in the sealed platinum container. (●): Co<sub>2</sub>Z, (◐): Ba-M, (▽): BaF<sub>2</sub> (■): Spinel ferrite.

**Fig. 8.** SEM photograph of the fractured surface of the 0 % glass added-specimen sintered at 1000°C for 10 h together with MgF<sub>2</sub> powder pellet in the sealed platinum container.

**Fig. 9.** Variations in the (a) real and (b) imaginary parts of the initial permeability of the 0 % glass added-specimen sintered at 1300°C for 1 h in air and the 5 % glass added-specimen sintered at 1000°C for 1 h in air as the function of frequency. Thick lines are the 5 % glass added-specimen and thin lines are the 0 % glass added-specimen.

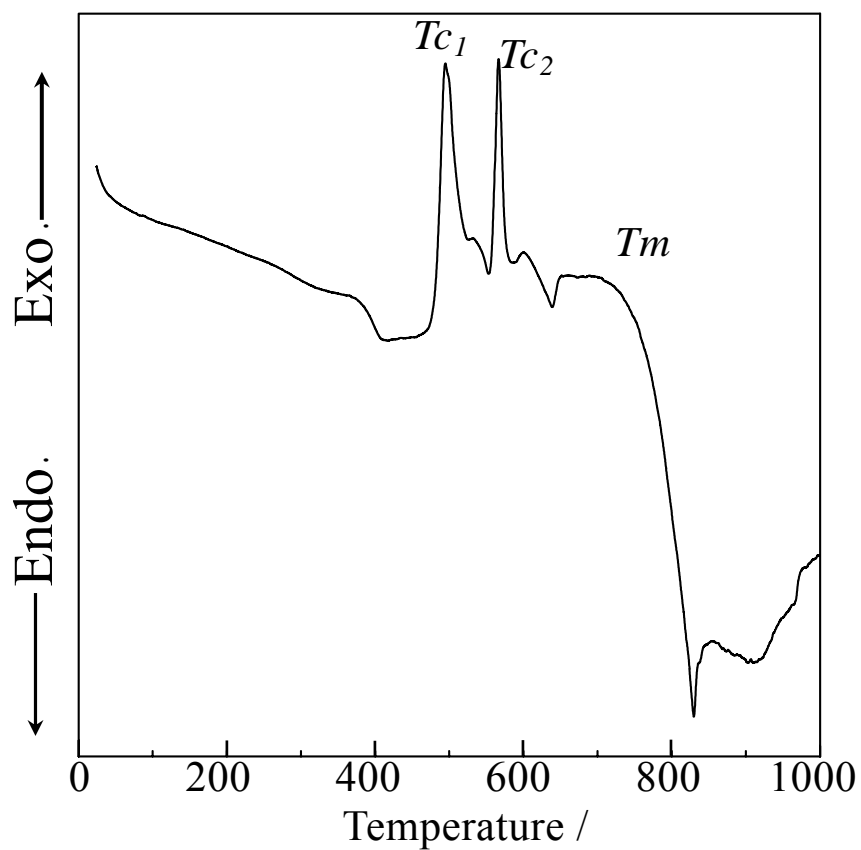
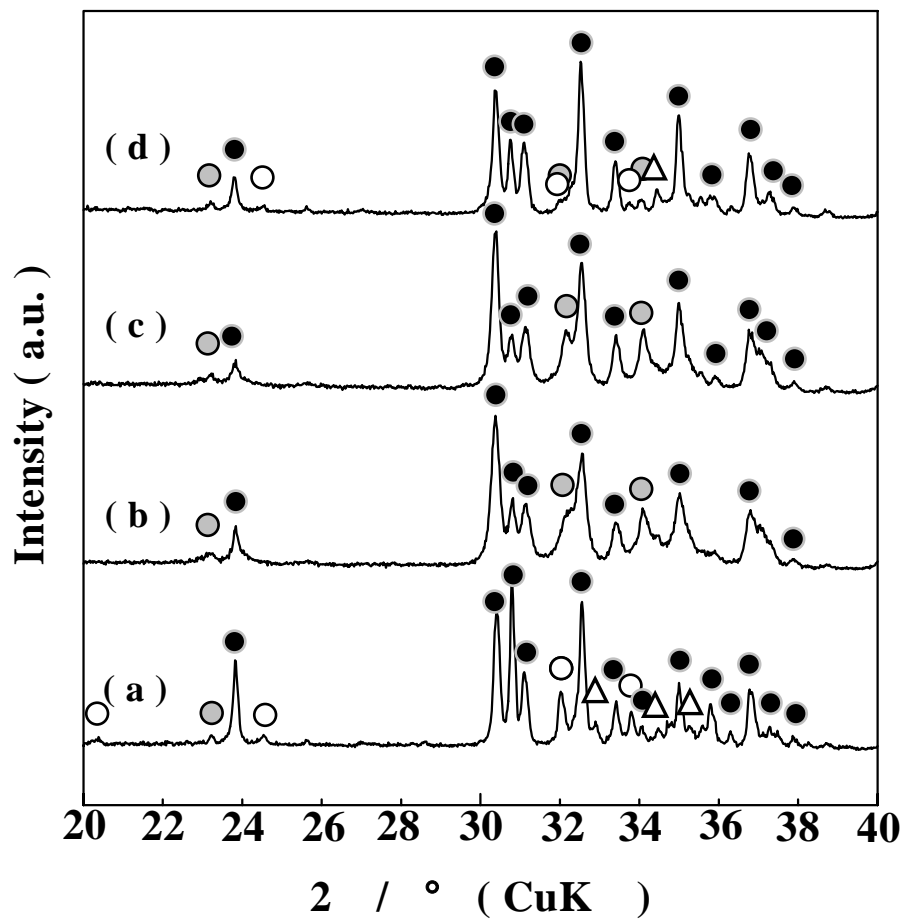
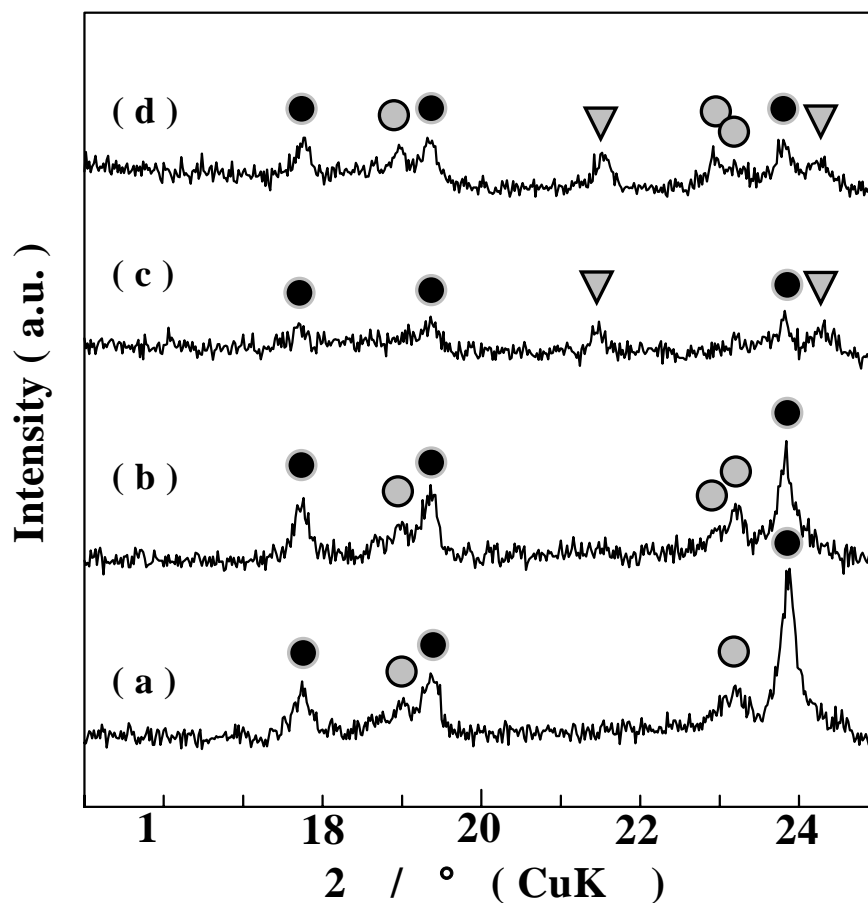


Fig. 1. DTA curve of the additive



**Fig. 2.** XRD patterns of (a) the as-calcined ferrite powder and the 0 % glass added-specimen sintered at (b) 1000°C for 1 h in air, (c) 1000°C for 10 h in the sealed platinum container and (d) 1300°C for 1 h in air. (●):  $\text{Co}_2\text{Z}$ , (◐): Ba-M, (○):  $\text{Co}_2\text{Y}$ , (Δ):  $\text{Co}_2\text{W}$ .



**Fig. 3.** XRD patterns of the 0 % glass added-specimen sintered at 1000°C (a) for 1 h in air and (b) for 10 h in the sealed platinum container and the 5 % glass added-specimen sintered at 1000°C (c) for 1 h in air and (d) for 10 h in the sealed platinum container. (●):  $\text{Co}_2\text{Z}$ , (●): Ba-M, (▼): Unknown.

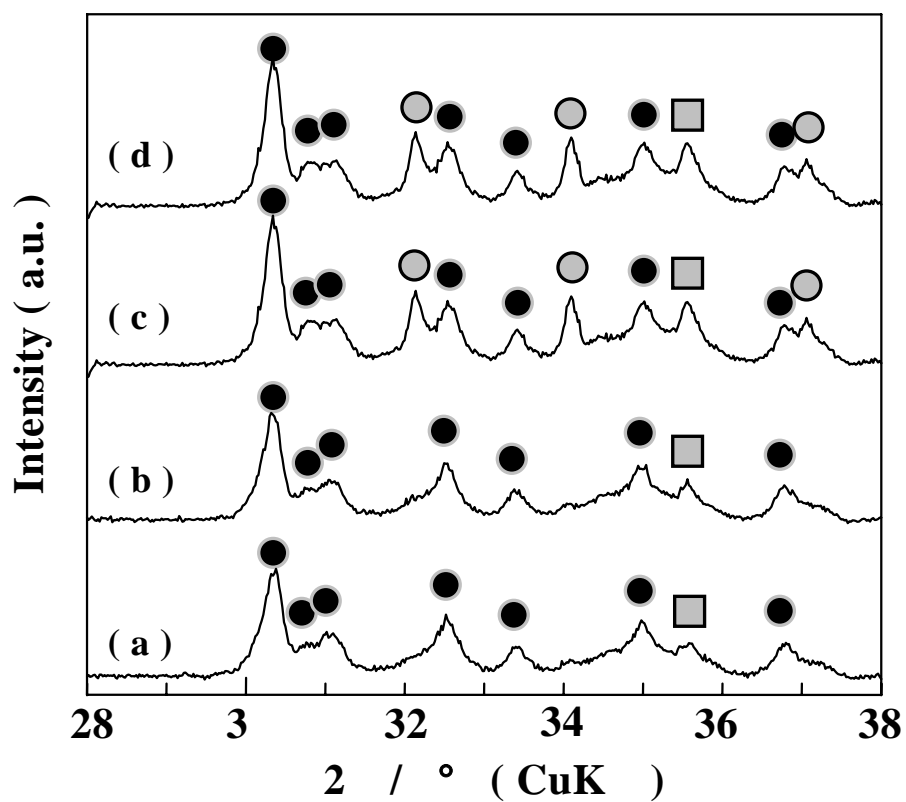


**Fig. 4.** XRD patterns of the 5 % glass added-specimen sintered at (a) 975°C for 1 h in air, (b) 1000 °C for 1 h in air, (c) 1000°C for 10 h in the sealed platinum container and (d) at 1050°C for 1 h in air. (●):  $\text{Co}_2\text{Z}$ , (○): Ba-M, (Δ):  $\text{Co}_2\text{W}$ , (■): Spinel ferrite.

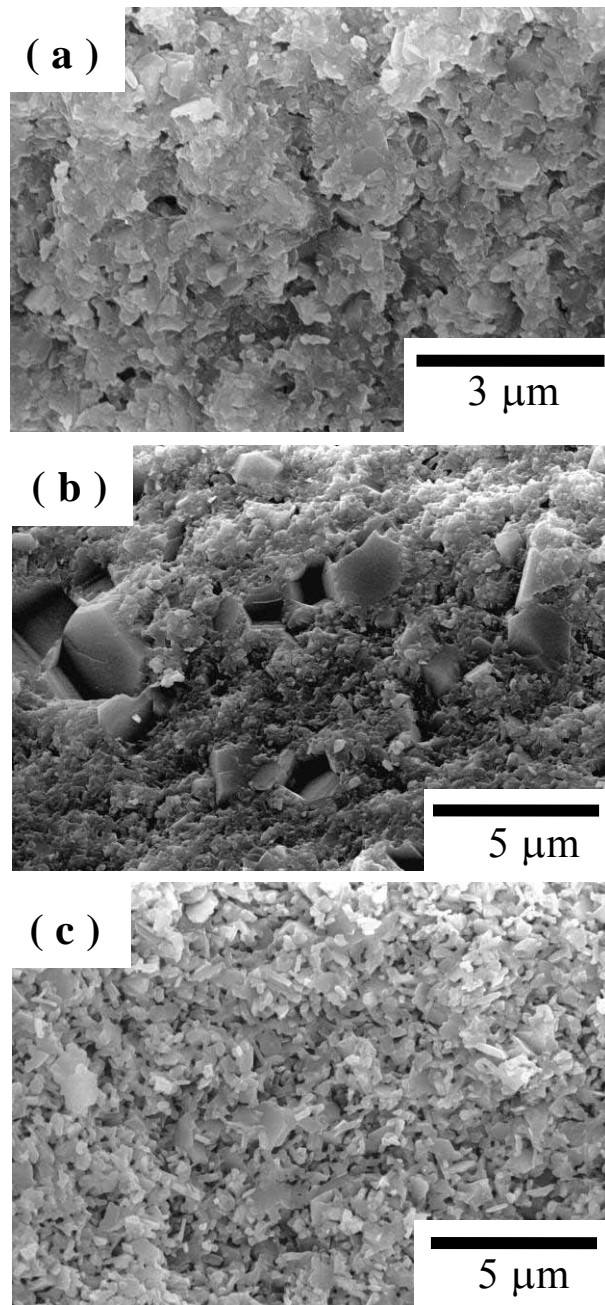


**Fig. 5.** SEM photographs of fractured surfaces of the 5 % glass added-specimen sintered at 1000°C (a) for 1 h in air, (b) for 10 h in the sealed platinum container and (c) the 0 % glass added-specimen sintered at 1000°C for 10 h in the sealed platinum container.



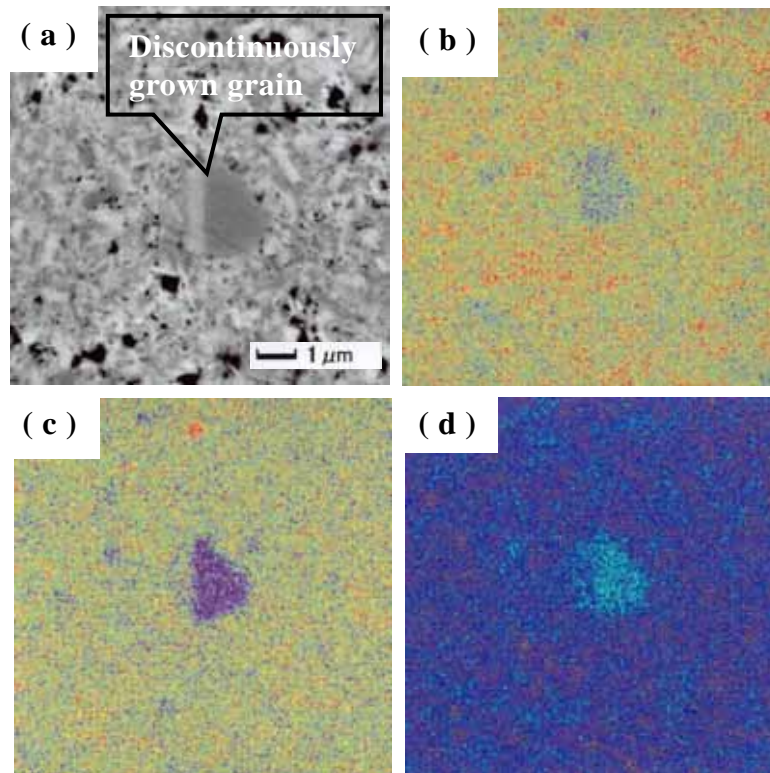


**Fig. 6.** (a) The reflection electron image of the polished surface of the 5 % glass added-specimen sintered at 1000°C for 10 h in the sealed platinum container. Distribution of (b) Ba, (c) Co and (d) Fe on the same surface of the sintered specimen. The contrast of (b), (c) and (d) means that the brighter part is richer in the element.

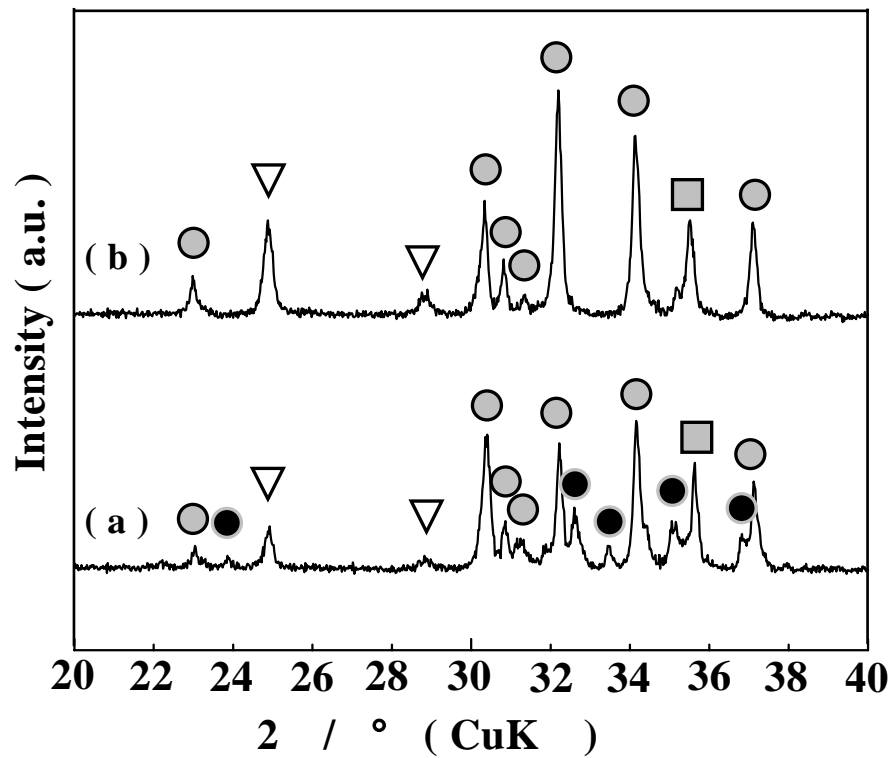


**Fig. 7.** XRD patterns of the 0 % glass added-specimen sintered at 1000°C for 10 h together with (a) the additive glass powder pellet and (b)  $\text{MgF}_2$  powder pellet in the sealed platinum container. (●):  $\text{Co}_2\text{Z}$ , (○): Ba-M, (▽):  $\text{BaF}_2$  (■): Spinel ferrite.

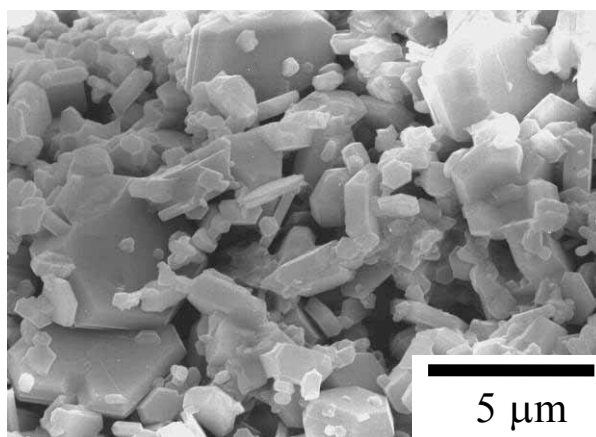


**Fig. 8.** SEM photograph of the fractured surface of the 0 % glass added-specimen sintered at 1000°C for 10 h together with MgF<sub>2</sub> powder pellet in the sealed platinum container.

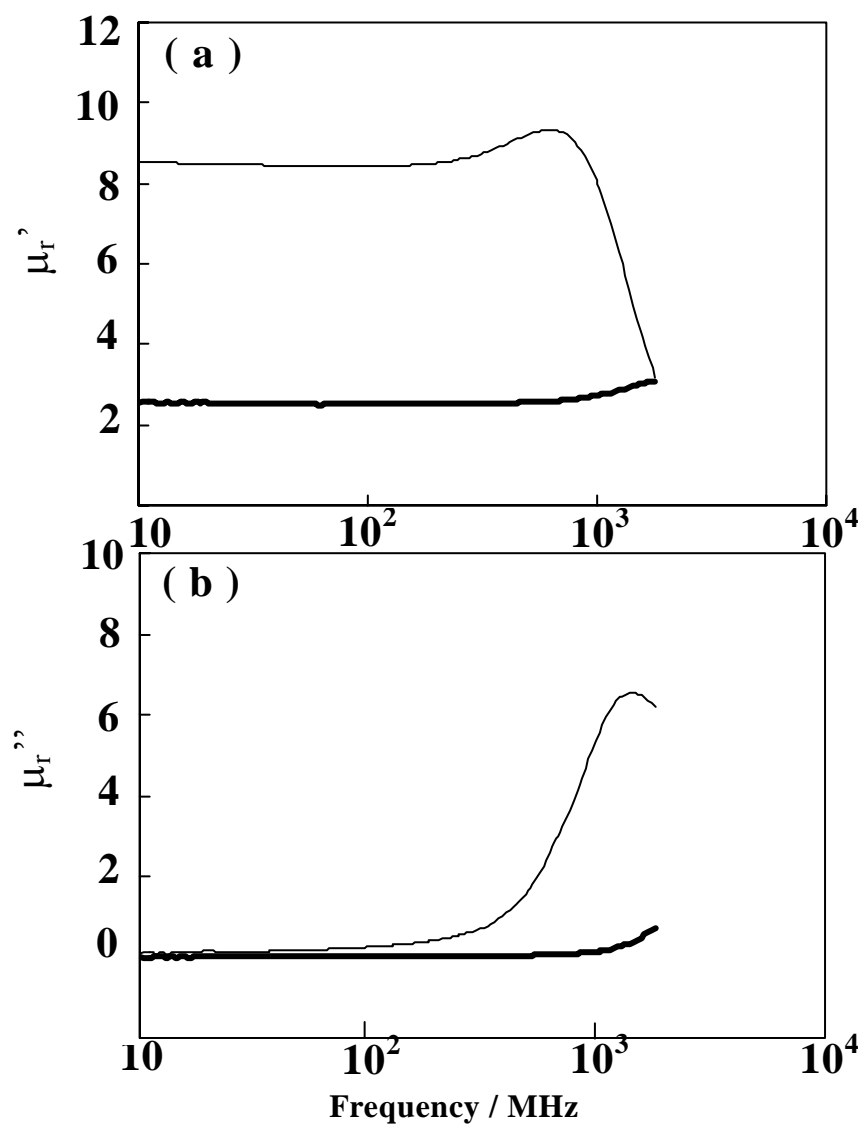


**Fig. 9.** Variations in the (a) real and (b) imaginary parts of the initial permeability of the 0 % glass added-specimen sintered at 1300°C for 1 h in air and the 5 % glass added- specimen sintered at 1000°C for 1 h in air as the function of frequency. Thick lines are the 5 % glass added-specimen and thin lines are the 0 % glass added-specimen.